Proceedings of the 17th International Conference on Manufacturing Systems – ICMaS
ISSN 1842-3183

University POLITECHNICA of Bucharest, Machine and Manufacturing Systems Department
Bucharest, Romania

SENSORLESS MONITORING OF CFRP DRILLING

Mehdi CHERIF, Pierrick LEGRAND

Abstract: *For the final assembly of aerostructure, drilling still remains a key operation. Drill wear is a serious concern in the CFRP drilling process because worn tool cause delamination, excessive roughness and uncut fiber at the exit of the hole. This paper presents signal analysis using wavelet approach for sensorless drilling monitoring based on spindle and feed current. The proposed methodology is tested on the drilling process of T800 M21 prepreg carbon with ϕ6.35mm carbide drill. The results point out the performance of the feed current proposed indicator rather than the spindle current for the drilling process monitoring of CFRP material.*

Key words: *CFRP drilling, tool wear, sensorless monitoring, signal analysis, wavelet.*

1. INTRODUCTION

In the aerospace industry, drilling account for 40% of all the material removal operation [1]. The monitoring of the drill wear is a key issue to avoid high cost workpiece damage during the final assembly. Many researchers proposed several approaches for the drilling monitoring mainly concerned with metal material [2]. During the CRFP drilling, the high temperature and abrasive effect of the carbon fiber induce rapid tool wear that modify the cutting process indicator such as cutting forces and torques. The thrust force and torque rise induce different damage on the drilled hole (delamination, excessive roughness etc.) [4, 5]. Those parameters can be monitored directly using force acquisition device or indirectly by the current from the spindle and the feed driver of the drilling machine. Spindle current and feed driver current are closely related to the cutting forces and torques [6]. Sensorless approaches are more easily integrated in the production process and don't need any extra device since spindle current and feed driver current are available directly in almost all the modern machinery. In this paper the evolution of the cutting indicator from both external measurement devices and built in device (CNC controller) are presented and analysed in the case of CFRP drilling with a carbide tipped drill. The evolution for 20 holes on thick CFRP (16.5 mm) of different cutting process indicators (forces, torque spindle current, feed driver current) is analysed. Several signal processing approaches are presented to define the most adapted indicator for CRFP online drilling monitoring for the aerospace industry.

2. THEORETICAL BACKGROUND

2.1. Wavelet analysis

In this work, we use a wavelet transform (see [7, 8]) in order to obtain the frequential content at each dyadic scale at any time. With this information, we'll estimate the noise (section 2.2) and the Hölder exponent (section 2.3). The continuous wavelet transform of a signal X is given by:

$$X(a,b) = \frac{1}{\sqrt{a}} \int_{-\infty}^{+\infty} X(t) \Psi\left(\frac{t-b}{a}\right) dt \,. \qquad (1)$$

In this expression, Ψ is the wavelet (a wave localised in time), a is a scale factor and b is a translation parameter (temporal shift). Variable a represents the inverse of the frequency: the smaller a the (temporally) narrower the wavelet (i.e. the analysing function). In this work we use a discrete wavelet transform which is faster than the continuous transform. The discrete wavelet transform can be obtained thanks to the discretization of the parameters of resolution (a) and position (b). One then has the following relation where $j = 1 \ldots.n$, n is the log 2 of the length of the signal and $k = 1..2\text{^}(j - 1)$.

$$X_{j,k} = \int_{+\infty}^{-\infty} X(t) \Psi\left(2^{-j} t - k\right) dt \,. \qquad (2)$$

2.2. Standard deviation estimation

This paragraph describes a way to estimate the standard deviation of an additive Gaussian noise. Suppose that one observes $Y = X + B$, a noisy signal obtained by summing an unknown original signal X and a Gaussian noise B. Since the impact of noise is more important on the high frequencies, Donoho and Al. in [9] use the wavelet coefficients at the finest level of resolution to estimate the standard deviation of B. Thus, we obtain the following formula:

$$\hat{\sigma} = \frac{\mathrm{MAD}}{0.6745} \qquad (3)$$

with

$$MAD = median_k\left(\left| y_{n,k} - median_p\left(y_{n,p}\right) \right|\right), \qquad (4)$$

where the median absolute deviation (MAD) is computed on the wavelet coefficients of the noisy signal at the finest level.

2.3 Hölder regularity analysis

This section focuses on the Hölder characterizations of regularity of the signal. To simplify notations, we assume that our signals are nowhere differentiable.

Definition: Pointwise Hölder exponent. Let $\alpha \in (0, 1)$, and $x_0 \in K \subset R$. A function f: $K \rightarrow R$ is in $C^{\alpha}{}_{x0}$ if for all x in a neighborhood of x_0:

$$\left| f(x) - f(x_0) \right| \leq c \left| x - x_0 \right|^{\alpha}, \qquad (5)$$

where c is a constant. The pointwise Hölder exponent of f at x_0, denoted $\alpha_p(x_0)$, is the supremum of the α for which the equation (5) holds. Various methods can be used in order to estimate the Hölder exponent. In this study, a wavelet-based method is used (see [10, 11]).

3. EXPERIMENTAL PROCEDURE

Drilling experiments were performed on a high speed machining center MIKRON HSM 600U. It is a 5 axis CNC machining with a ITNC 530 control with the following specifications:

The machined material is a T800 M21 Carbon Fiber prepreg carbon tape (UD 200 gr/m^2) with a total thickness of 16.5 mm (129 plies × 0.128 mm/ply). The tool used is a uncoated carbide drill made by Diager Industrie with a 120 degrees point angle. Due to the aeronautical industry specification, no coolant was used during the cutting process. During the experiment two different ways of monitoring the cutting forces were used (see Fig. 1). The first one is based on the scope function directly on the controller Heidenhain ITNC530. This functionality allows us to save numerous information (spindle current, feed current, electrical and mechanical power consumption etc.) directly from the machine controller. The second methodology used for the monitoring is based on cutting forces and moment dynamometer. As the current feed and spindle can be related to thrust forces and torque [3], the presented analysis is only proposed for the sensorless approach (using the integrated scope function of the CNC) and based on the spindle current and feed driver current.

Table 1

Specifications of the CNC HSM600U

Rotation Speed	Feed rate	Nominal power (S1)	Nominal Torque
36000 rpm	40 m/min	32 kW	16 Nm

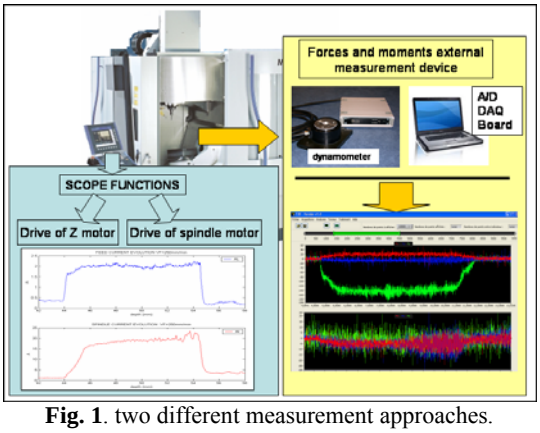

Fig. 1. two different measurement approaches.

Figure 2 presents the general profile for the feed current and the spindle current during the CFRP drilling sequence. The first part of the signal ([*AB*] corresponds to the approach, during the entrance and the cutting sequence [*BC*], both feed and spindle current increase until the bottom of the test part is reached [*CD*]. during the exit sequence, the tool still moves forward [*DE*] until the end of the drilling sequence [*EF*]. The tool remains 2 seconds at the bottom of the drill before coming out backward.

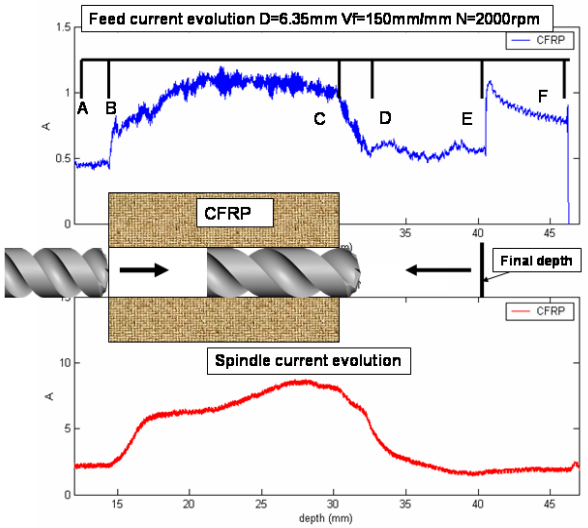

Fig. 2. Drilling sequence analysis.

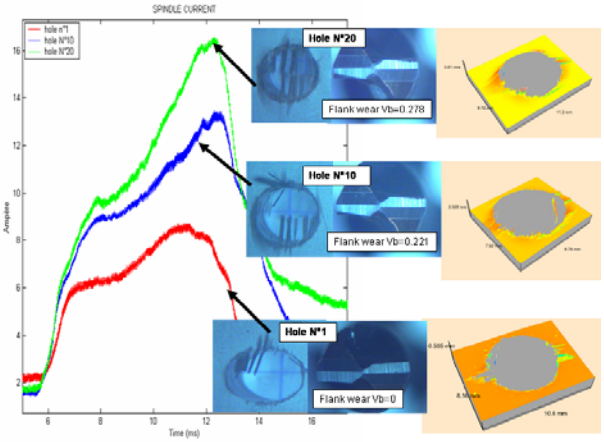

Fig. 3. Evolution of the spindle current.

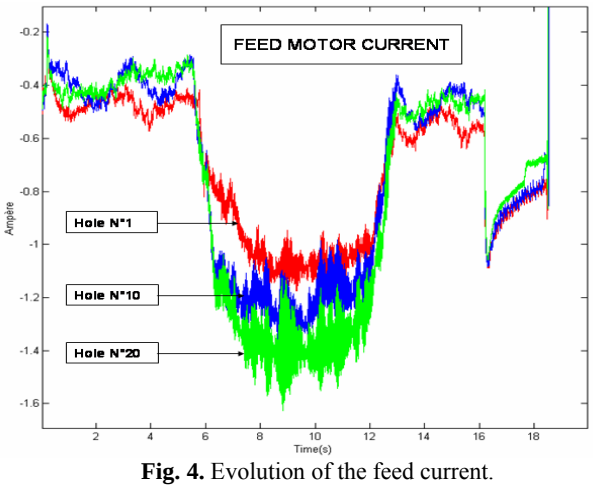

Fig. 4. Evolution of the feed current.

3.1. Influence of the tool wear on the spindle and feed current

Figures 3 and 4 present the evolution of the spindle current and the feed current due to tool wear corresponding to 20 holes. The cutting condition used are cutting speed of 40 m/min (N = 2000 rpm) and a feed of 150 mm/min. In the right part of the Fig. 3 the 3D rugosimeter measurement of the exit surface around the hole presents delamination due to the excessive feed force.

4. SIGNAL ANALYSIS

In this section, we apply the tools described in section 2 in order to propose the most adapted indicator for tool wear monitoring during the drilling process. We use some algorithms implemented in the toolbox FracLab (see [12, 13]). Results are illustrated on the six following illustration. The X axis represents the drilled hole number. Table 2 presents the correlation between the tool wear rate (via the hole number) and the evolution of differents indicators based on spindle and feed current signal analysis. For the current feed drive (first row), power, median and noise level are closely related to tool wear and can easily be used for the definition of tool wear monitoring. Hölder function does not give significant result. In the second row, the power, median and mean Hölder function give good correlation with the tool wear evolution. Based on the spindle current, noise signal analysis is not correlated with the tool wear state.

5. CONCLUSIONS

This paper presents the analysis of different indicators for the monitoring of tool wear during CFRP drilling. During the tool wear process produced by the highly abrasive carbon fiber, both spindle current and feed current are modified. Excessive tool wear produces important thrust forces that induce delamination and uncut fiber on CFRP part. The high cost of the machined part needs improved methodology for the tool wear monitoring with sensorless approaches (in particular, no dynameter equipment on the part). This study points out the sensibility of different indicators obtained from signal analysis (power, median level) and wavelet approach (noise and mean Hölder function), in relation with the tool wear level.

Finally, it would be useful to develop a tool monitoring algorithm based on the present study to improve the effectivness of the monitoring system on drilling machine dedicated to CFRP drilling. The combination of the different presented indicators should lead to a robust monitoring system.

Table 2

Correlation results with the hole number

Signal / Current	Power indicator	Median indicator	Noise indicator	Hölder function
Feed current	0.98113	0.9447	0.955	0.5089
Spindle current	0.9059	0.8616	-0.2078	0.826

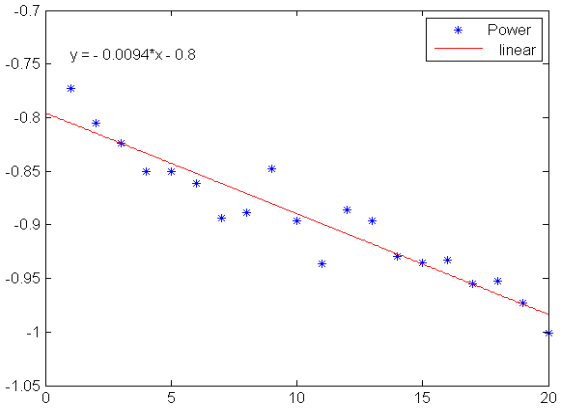

Fig. 5. Power evolution for the feed current.

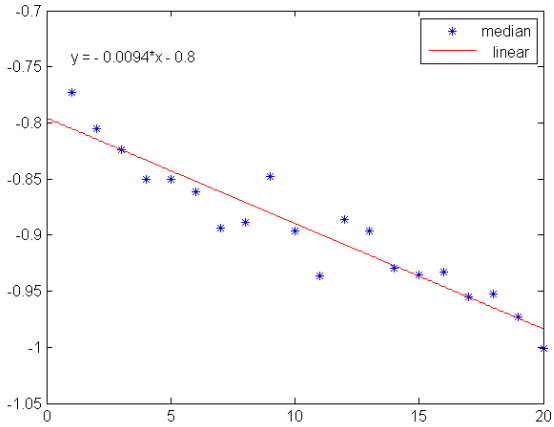

Fig. 6. Median evolution for the feed current.

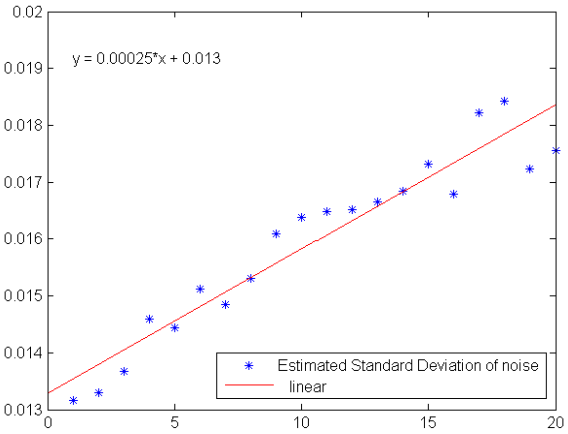

Fig. 7. Noise evolution for the feed current.

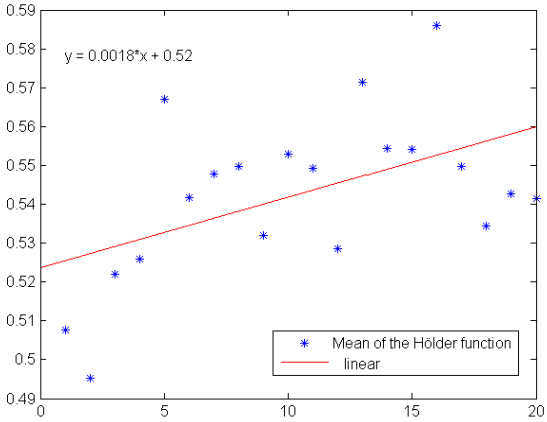

Fig. 8. Hölder function evolution for the feed current.

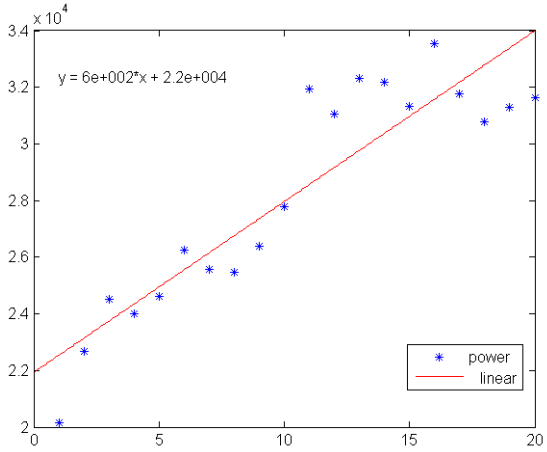

Fig. 9. Power evolution for the spindle current.

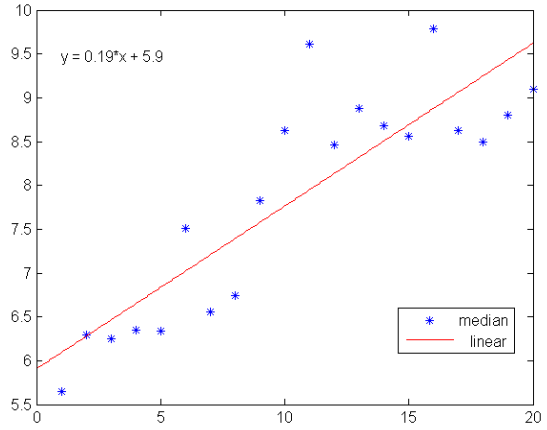

Fig. 10. Median evolution for the spindle current.

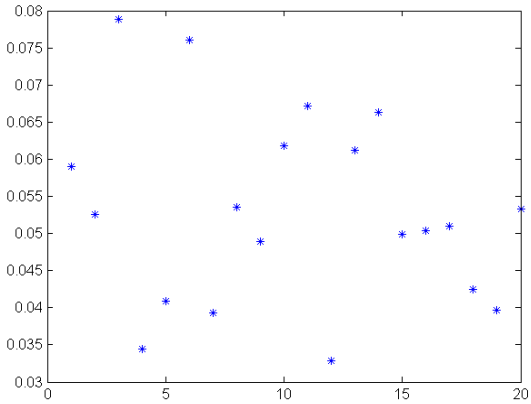

Fig. 11. Noise evolution for the spindle current.

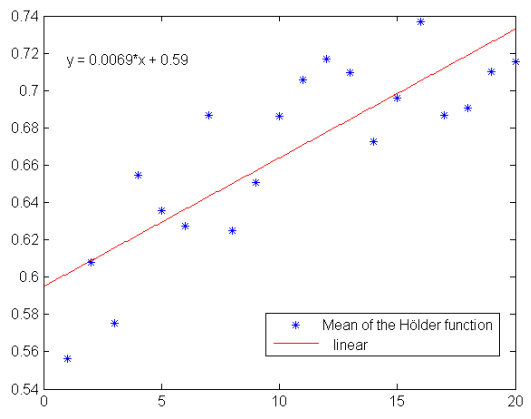

Fig. 12. Hölder function evolution for the spindle current.

REFERENCES

[1] Tsao, C.C., Hocheng, H. (2007). *Effect of tool wear on delamination in drilling composite materials*, International Journal of Mechanical Sciences, Vol. 49, Issue 8, August 2007, pp. 983-988.

[2] Roudge, M., Cherif, M., Cahuc, O., Darnis, P. , Danis, M. (2008). *Multi-layer Materials. Qualitative Approach of the Process*, International Journal of metal forming.

[3] Jantunen, E. (2002). *A summary of methods applied to tool condition monitoring in drilling*, International Journal of Machine Tools and Manufacture, Vol. 42, Issue 9, July 2002, pp. 997-1010.

[4] Pena, B., Aramendi, G., Rivero A., Lopez de Lacalle, L.N. (2005). *Monitoring of drilling for Burr detection using spindle torque,* International Journal of Machine Tools and Manufacture, Vol. 45, Issue 14, November 2005, pp. 1614-1621.

[5] Abrao, A.M. , Faria , P.E., Campos Rubio, J.C., Reis, P. , Paulo Davim, J. (2007). *Drilling of fiber reinforced plastics: A review,* Journal of Materials Processing Technology, Vol.186, Issues 1-3, May 2007, pp 1-7.

[6] Franco-Gascaa, L. A., Herrera-Ruiza, G. , Peniche-Veraa, R., Jesus Romero-Troncosob, R., Leal-Tafolla, W. (2006). *Sensorless tool failure monitoring system for drilling machines*, International Journal of Machine Tools and Manufacture, Vol. 46, Issues 3-4, March 2006, pp. 381-386.

[7] Meyer, Y. (1990). *Ondelettes et operateurs*. Actualités Mathématiques, [Current Mathematical Topics], Hermann, Paris, 1990.

[8] Daubechies, I. (1992). *Ten Lectures on Wavelets,* CBMS-NSF Lecture Notes nr. 61, SIAM, 1992.

[9] Donoho, D.L., Johnstone, I.M. (1994). *Ideal spatial adaptation by wavelet shrinkage,* Biometrika, Vol 81, pp. 425–455.

[10] Jaffard, S. (2004). *Wavelet Techniques in Multifractal Analysis, Fractal Geometry and Applications: A Jubilee of Benoit Mandelbrot*, M. Lapidus et M. van Frankenhuijsen Eds., Proceedings of Symposia in Pure Mathematics (AMS) Vol. 72, Part 2, pp. 91-151.

[11] Legrand, P. (2004). *Débruitage et interpolation par analyse de la régularité Höldérienne. Application à la modélisation du frottement pneumatique/chaussée*, PhD Thesis, University of Nantes, Ecole Centrale de Nantes. December 2004.

[12] *** *FracLab: a software toolbox for fractal processing of signals*. `http://apis.saclay.inria.fr/FracLab/.`

[13] Lévy Véhel, J., Legrand, P. (2004). *Signal and image processing with FracLab*, FRACTAL04, Complexity and Fractals in Nature, 8th International Multidisciplinary Conference, Vancouver, Canada, April 4-7.

Authors:

Mehdi CHERIF
LGM2B, University of Bordeaux 1, France
E-mail: `mehdi.cherif@u-bordeaux1.fr`

Pierrick LEGRAND
IMB, Institut de mathématiques de Bordeaux, UMR CNRS 5251, University of Bordeaux 2, France,
E-mail: `Legrand@sm.u-bordeaux2.fr`